SLAC–PUB–9995
DAPNIA/SPP 95-18
CERN Libraries, SCAN 9509150
September 1995

BaBar: A new detector for studying CP violation in the B system*

R. Aleksan
DAPNIA/SPP, Center d'Etudes Nucleaires, Saclay
F-91191 Gif-sur-Yvette Cedex, France

On behalf of the BaBar Collaboration

Presented at the Second Workshop for Physics and Detectors for DAFNE
Frascati, Italy
April 4-7, 1995

* Work supported in part by Department of Energy contract DE–AC03–76SF00515.

BABAR: A NEW DETECTOR FOR STUDYING CP VIOLATION IN THE B SYSTEM.

R. Aleksan[1]
DAPNIA/SPP, Centre d'Etudes Nucléaires, Saclay,
F-91191 Gif-sur-Yvette Cedex, France

September 4, 1995

Abstract

A new detector for investigating the CP violation mechanism in the B meson system is being built and is scheduled to take data at PEP II, the asymmetric B Factory in construction at SLAC, at the end of this century. Its main characteristics are briefly overviewed in this paper. Its sensitivity for measuring CP violation in some selected B decays is also discussed, underlining the great potential of this detector to accomplish a comprehensive study of this phenomenon.

1 – Introduction

In order to explain why the observed universe is matter dominated, it is necessary to create a mechanism which allows one to distinguish matter from antimatter. This is accomplished together with a few other conditions by introducing the non-conservation of the CP symmetry in the theory describing the interactions between the particles at the early stage of the universe[1]. At the turn of the century, we should begin to understand the origin of the CP violation phenomenon observed 30 years ago by J.H. Christenson, J.W. Cronin, V.L. Fitch and R. Turlay[2] as *BABAR*, the new proposed detector at the PEP II asymmetric e^+e^- B Factory of SLAC, will record its first data at the $\Upsilon(4S)$ resonance where pairs of B mesons are produced. The expression "asymmetic B Factory" is used to designate a facility which has two beams with different energies in order to give a longitudinal boost to the center of mass system and which is able to deliver a very high luminosity ($\mathcal{L} \geq 3 \times 10^{33} cm^{-2} s^{-1}$).

The *BABAR* detector[3], a schematic view of which is shown in figure 1, has been designed by a large international collaboration consisting of about 480 physicists and engineers from 10 countries (Canada, China, France, Germany, Italy, Norway, Russia, Taiwan, UK and US). It will instrument the unique interaction region of PEP II and is scheduled to be operational by year 1999, about six months after the startup of the collider foreseen in the fall 1998.

[1] on behalf of the *BABAR* Collaboration

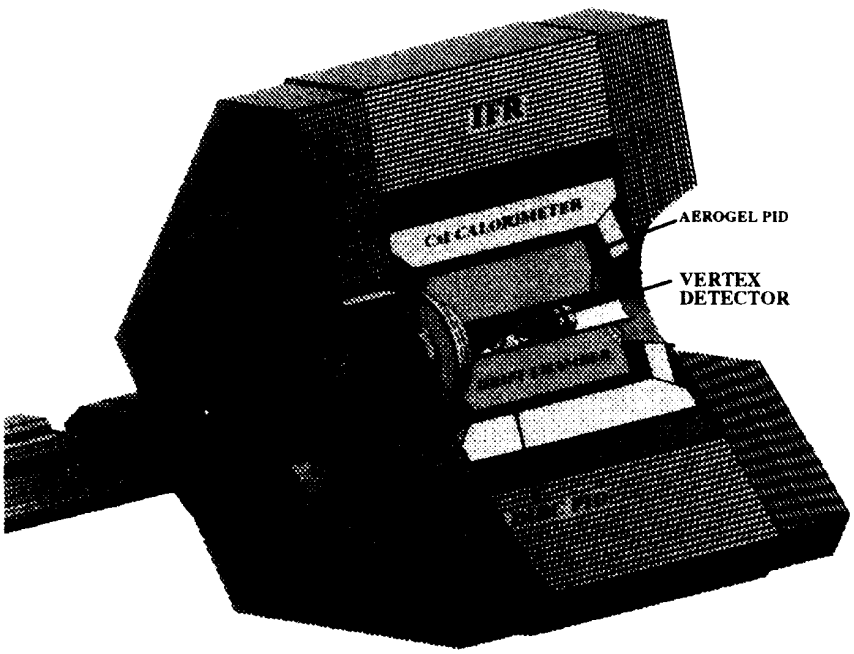

Figure 1: Schematic view of the *BABAR* detector

2 – CP violation in the B system

In the Standard Model (SM) of the fundamental interactions [SU(3)×SU(2)×U(1)], all CP non-conserving phenomena are induced through the interference of processes involving different "Weak" phases. These phases are generated by the mixing of the quark flavors via the charged weak currents, $W^{\pm}$, providing that a minimun of 3 fermion families exist. In this framework, the Cabibbo mixing 2×2 matrix[4] can be extented to a more general $n \times n$ matrix. If only 3 families of fermions exist as indicated by LEP data[5], only 3 mixing angles and one phase, δ, are necessary to describe the corresponding unitary 3×3 matrix as proposed by Kobayashi and Maskawa[6]. A useful approximation of the CKM matrix has been proposed by Wolfenstein[7].

$$V_{CKM} = \begin{pmatrix} V_{ud} & V_{us} & V_{ub} \\ V_{cd} & V_{cs} & V_{cb} \\ V_{td} & V_{ts} & V_{tb} \end{pmatrix} = \begin{pmatrix} 1-\frac{\lambda^2}{2} & \lambda & A\lambda^3(\rho - i\eta) \\ -\lambda & 1-\frac{\lambda^2}{2} & A\lambda^2 \\ A\lambda^3(1-\rho-i\eta) & -A\lambda^2 & 1 \end{pmatrix} + \mathcal{O}(\lambda^4) \qquad (1)$$

Here, the parameter $\lambda = 0.2205$ is the sine of the Cabibbo angle while $A = 0.82 \pm 0.04$ is deduced from the measurements of V_{cb}[8] and ρ and η are in the range 0 to 1/2[9]. From the various unitarity relations which can be derived, a particularly interesting one connects CKM elements related to B physics:

$$V_{ub}^{*} - \lambda V_{cb} + V_{td} \simeq 0 \qquad (2)$$

This equation represents the so-called "unitarity triangle" in which the lengths of the sides are of the same order, see figure 2.

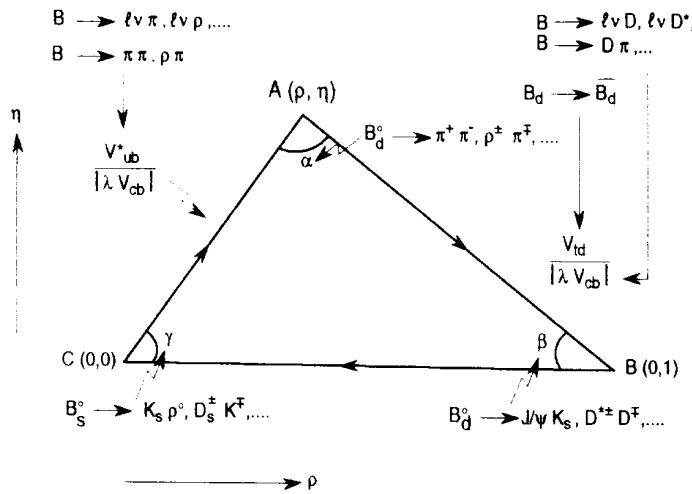

Figure 2: The unitarity triangle. Some B decay modes which are relevant for the sides and angles measurements are also indicated.

The ultimate goal of the *BABAR* detector is to observe CP violation in the B meson system in a large variety of modes. This systematic study should allow us to get either a comprehensive understanding of this phenomenon in the framework of the Standard Model or eventually explore a new domain. CP violation should manifest itself as a time dependent asymmetry in some B decays. A simple, although not exclusive, laboratory is provided by final states which are also CP eigenstates. The measured asymmetry is then directly related to the angle $\Phi = \alpha$, β or γ of the unitarity triangle as shown by the following equations.

$$Pr(\overset{(-)}{B^0} \rightarrow f_{CP}) = \frac{e^{-\Delta t/\tau}}{\tau}\left(1 \overset{(-)}{+} \eta_{CP} \sin 2\Phi \sin x_d \Delta t/\tau\right) \tag{3}$$

where $x_d = (m_{B_1^o} - m_{B_2^o})\tau \simeq 0.735 \pm 0.045$[9] and Δt is the decay time of the second B meson after the decay of the first one has occured. This quantity is derived through the measurement of the distance between both B decays using $\Delta t \simeq m_B \Delta z / E_B c$. In the formula above, B_1^o and B_2^o are the B_d^o mass eigenstates. Finally, η_{CP} (± 1) is the CP parity of the final state and m_B, E_B and τ are the B_d^o mass, energy and lifetime respectively.

Many B decay modes involving J/ψ and kaons, D-meson pairs and light meson pairs have been studied with detailed Monte Carlo to extract the parameters sin2β and sin2α which are directly connected to the value of the phase δ. The sensitivity to sin2β and sin2α are expected to be 0.059 and 0.09 respectively after 1 year of operation of *BABAR* at PEP II during which an integrated luminosity of 30 fb^{-1} is expected. Table 1 gives a summary of the modes which have been considered together with

Final State	Br	Φ	$\delta(\sin 2\Phi)$
$J/\psi K^0_S$	0.5×10^{-3}	β	0.098
$J/\psi K^0_L$	0.5×10^{-3}	β	0.16
$J/\psi K^*$[10]	1.6×10^{-3}	β	0.19
Sum J/ψX		β	0.076
D^+D^-	6×10^{-4}	β	0.21
$D^{*+}D^{*-}$[11]	7×10^{-4}	β	0.15
$D^{*\pm}D^{\mp}$[11]	8×10^{-4}	β	0.15
Sum D D		β	0.095
Combined		β	0.059
$\pi^+\pi^-$	1.2×10^{-5}	α	0.20
$\rho\pi$[12]	5.8×10^{-5}	α	0.11
$a_1\pi$[12]	6×10^{-5}	α	0.24
Combined		α	0.09

Table 1: Expected errors on the measurement of $\sin 2\Phi$ from various channels with 30 fb^{-1}. The assumed branching fractions and the measured angle are also indicated.

their "CP reach". Figure 3 shows how these errors compare with the present allowed region obtained by the measurement of the sides of the triangle. A significant improvement of the errors on the sides is also expected, constraining further the triangle and leading together with the angle measurements to a powerful consistency test of the SM in a yet very obscure sector of the theory.

3 – The *BABAR* detector

High performance and robust detectors are needed to accomplish this program successfully. The observation of CP asymmetries requires in particular:

- a precise measurement of the distance between the 2 B meson decays (of the order of 250 μm for beam energies of 9 GeV against 3.1 GeV as planned at SLAC)
- an efficient and relatively pure tagging of the flavor of the B which is not fully reconstructed. Electrons, muons and Kaons will be used for this purpose
- a large acceptance, a good efficiency and excellent particle identification for the modes which need to be fully reconstructed.
- a good momentum and energy resolution for the charged and neutral particles in order to reject the combinatorial background.

The *BABAR* detector has indeed been optimized [3] to fulfill the above criteria. It uses whenever possible well established technologies such as a silicon vertex detector[13], a central drift chamber, a Cesium Iodide Calorimeter[14] and Resistive Plate Chambers[15] for the intrumented flux return. Only the particle identification system uses new techniques since no currently used method is able to satisfy

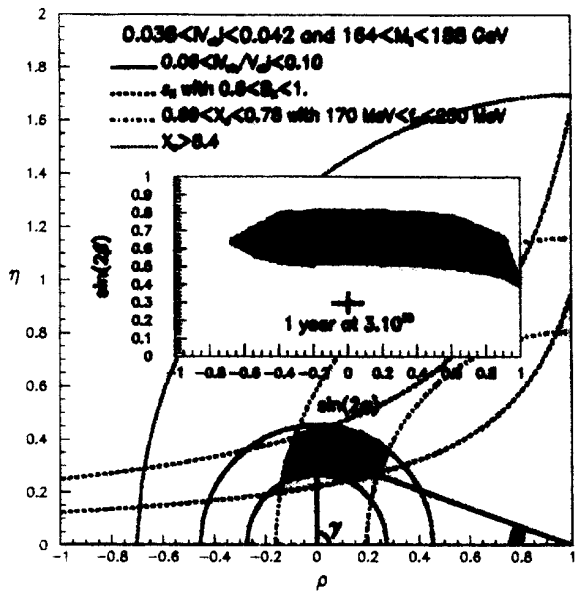

Figure 3: Present constraints of the unitarity triangle in the complex plane (ρ, η). The corresponding region for $\sin 2\beta$ versus $\sin 2\alpha$ is also shown.

our required needs. The dimension, acceptance and the expected performances of the individual subdetectors are summarized in the table 2.

In the following, we give a brief overview of the main features of the various subdetectors.

3.1 The silicon vertex detector

The distance between both B decays (fig. 4) is measured by means of a double silicon vertex detector with strips running parallel and perpendicular to the beam direction. Five layers of silicon detector

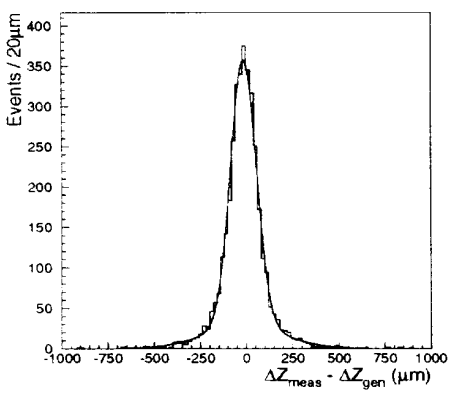

Figure 4: Resolution in Δz for $B^o \rightarrow \pi^+\pi^-$ with a primary lepton tag.

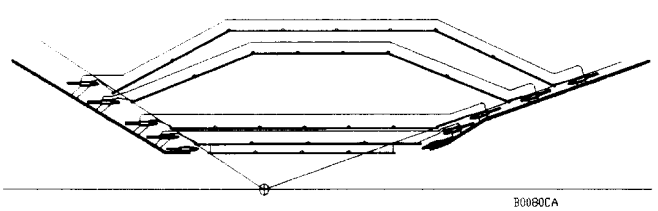

Figure 5: A view of the vertex detector in a plane containing the beam axis.

(fig. 5) at a radius extending from 3.2 to 14.4 cm from the interaction region are used for sufficient

Detector	Dimensions	Performance
Double-sided Silicon Strip detector	5 Layers $r = 3.2 - 14.4$cm $-0.87 < \cos\theta < 0.96$ $\sim$ 150000 channels	$\sigma_z = \sigma_{xy} = 50\,\mu\text{m}/p_t \oplus 15\,\mu\text{m}$ $\sigma_\phi = \sigma_\theta = 1.6\,\text{mr}/p_t$
Small Cell Drift Chamber	40 Layers $r = 22.5 - 80.0$cm $-111 < z < 166$cm $\sim$ 7000 channels	$\sigma(p_t)/p_t = [0.21\% + 0.14\% \times p_t]$
DIRC Cherenkov light imaging PID	$1.75 \times 3.5\,\text{cm}^2$ quartz $-0.84 < \cos\theta < 0.90$ $\sim$ 13400 channels	$N_{pe} = 20 - 50$ $\gtrsim 4\sigma$ K/π separation for all B decay products
Aerogel Threshold counter PID	n=1.006, 1.055 $0.916 < \cos\theta < 0.955$ $\sim$ 140 channels	$N_{pe} = 10$ π/K separation up to 4.3 GeV/c
CsI(Tl) Calorimeter	$16 - 17.5\ X_0$ $\sim 4.8 \times 4.8$cm crystals $\sim$ 6800 channels	$\sigma_E/E = 1\%/E(\text{GeV})^{\frac{1}{4}} \oplus 1.2\%$ $\sigma_\theta = 3\,\text{mr}/\sqrt{E(\text{GeV})} \oplus 2\,\text{mr}$
Superconducting coil and segmented iron	IR=1.40 m L = 3.85 m	$B = 1.5$T
RPC instrumented flux return	16–17 Layers $\sim$ 42000 channels	$\epsilon_\mu > 90\%$ for $p_\mu > 0.8$ GeV/c

Table 2: Summary of the main parameters of the *BABAR* detector (all angles are in the laboratory).

redundancy and to perform an efficient tracking of the soft pions over 91% of the solid angle. The total surface of silicon detector needed is about one m^2 with a longest strip dimension of about 24 cm. In order to minimize the multiple scattering, all the electronics is located outside of the acceptance of the detector by carrying the signals out by means of thin capton foils. This technique has already been tested succesfully.

3.2 The central drift chamber

Charged particle tracking is achieved in the central drift chamber with a total of 40 layers of axial and stereo wires . The inner and outer radii are 22.5 cm and 80 cm respectively. In order to ensure a very good single cell efficiency and low occupancy, a geometry with small cells (width $\simeq$ 1.8 cm) has been adopted. The momentum of the charged particles which are generated in B decays and reconstructed in the drift chamber is in the range 0.1-4.5 GeV/c. High resolution (fig. 6) is obtained by operating the chamber in a magnetic field of 1.5T generated by a superconducting solenoid. To improve further the momentum resolution, the multiple scattering is reduced by using a low Z gas[16, 17] such as He:i-C_4H_{10} 80:20. Cosmic tests with this type of gas have shown that excellent single cell resolution can be achieved ($\sigma \simeq 120 - 140\ \mu m$ on average) (fig. 7).

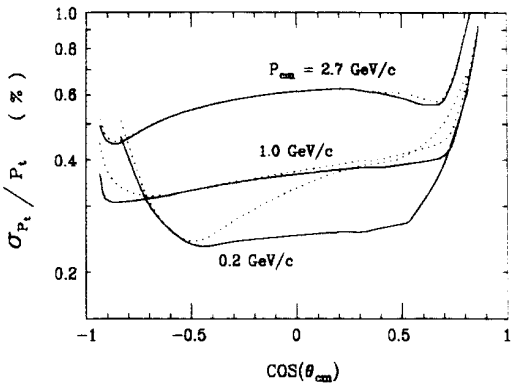

Figure 6: Transverse momentum resolution versus the center of mass angle. The dotted curve show the total momentum resolution (σ_p/p) assuming a 100 μm vertex constraint.

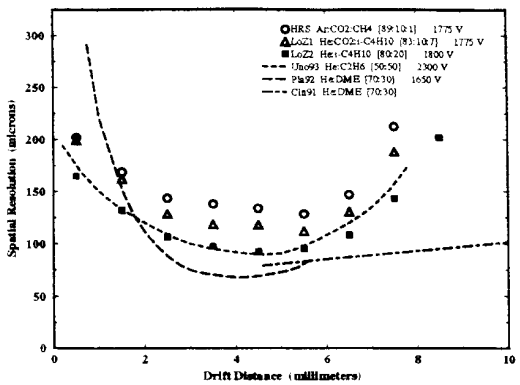

Figure 7: Single cell resolution for different gas mixture measured in a prototype chamber. Curves are the results of studies done elsewhere.

3.3 The particle identification system

Particle identification is one of the key elements of this detector. It is necessary to obtain a good effective tagging efficiency. Electron identification is done with the combination of the CsI calorimeter (see below) and the drift chamber. Muons are identified down to 0.5 GeV/c by instrumenting the flux return with 17 layers of Resistive Plate Chambers. This fine segmentation allows one in addition to identify K_L, increasing thus the sensitivity to $\sin(2\beta)$. Finally Kaon identification is achieved over 90% of the solid angle with dedicated detectors based on the observation of Čerenkov light. A novel technique (DIRC[18]) is used in the barrel region (fig. 8). It is based on the collection of Čerenkov

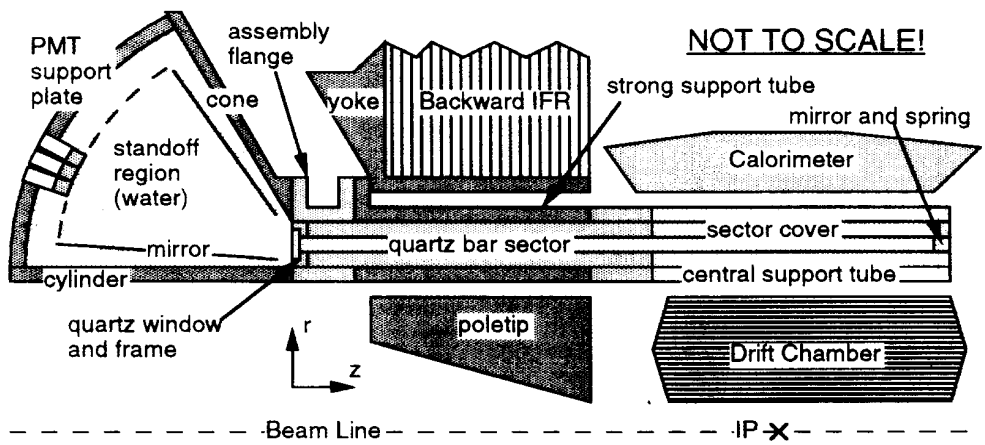

Figure 8: Schematic view of the DIRC (not to scale).

light produced by the particle traversing quartz bars. The light is internally reflected in the 4.8 m

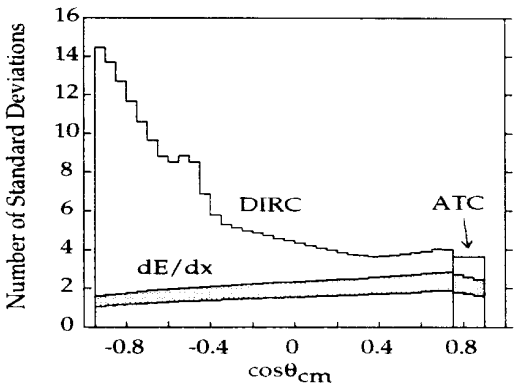

Figure 9: π/K separation for pions from $B \to \pi^+\pi^-$ as a function of the polar angle of the most energetic pion using DIRC and Aerogel. The shaded region shows the separation using dE/dx only.

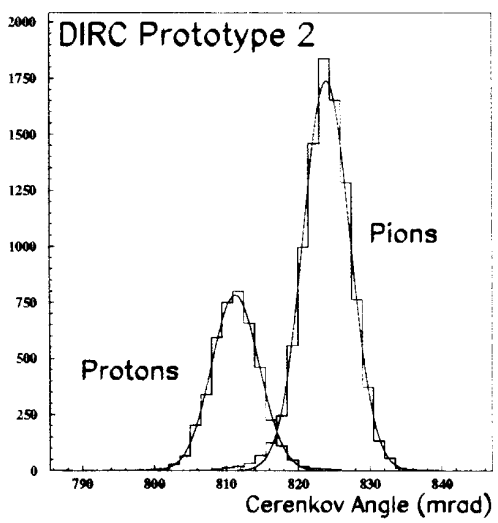

Figure 10: π/p separation at p=5.4 GeV/c (corresponding to π/K separation at 2.7 GeV/c) as obtained from a beam test using a detector equivalent to a quarter of the final device.

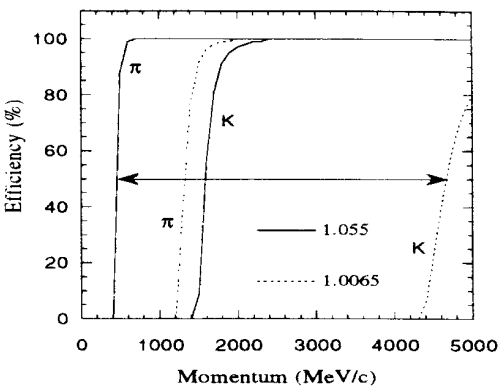

Figure 11: Threshold curve for pions and kaons as a function of momentum for the two aerogel index.

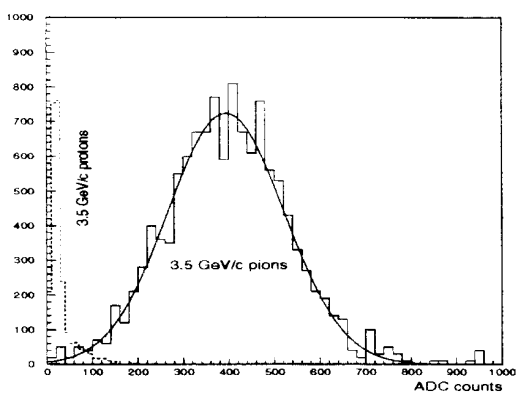

Figure 12: Responses of a prototype 1.0085 aerogel counter to 3.5 GeV/c pions (solid line) and the below threshold protons using a fine mesh tube in a 1.3T magnetic field.

long bars and detected outside of the flux return on an array of about 13000 phototubes allowing one to reconstruct the image of a truncated Čerenkov cone. A striking particularity of this device is the increase of the number of photoelectrons as the tracks are going toward the forward direction, giving a good π/K separation over the full acceptance of the detector for the most energetic particles produced in B decays such as in the reaction $B \to \pi^+\pi^-$ (fig. 9). Most recent beam tests at CERN[19] have confirmed the promising potential of such a detector (fig. 10). In the forward region, the Kaon identification is performed using Aerogel Threshold Counters (ATC) with a combination of two different indices (n_1=1.0065 and n_2=1.055) (fig. 11) possibly readout by fine mesh photomultipliers or hybrid photodiodes. Beam test results have established the proof of principle of such a detector as can be seen from fig. 12.

3.4 The CsI calorimeter

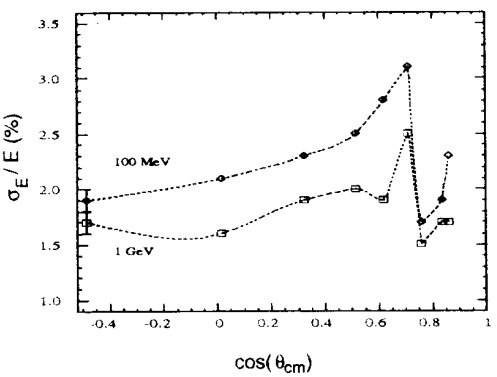

Figure 13: Single photon energy resolution as a function of the polar angle for E_γ = 0.1 and 1.0 GeV.

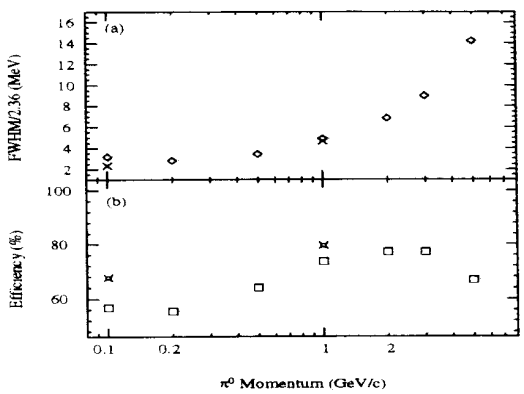

Figure 14: (a) Mass resolution and (b) efficiency for π^o generated at $\cos\theta_{cm} = 0^o$ vs the π^o energy. The crosses indicate the performance with no material in front of the calorimeter.

The average photon energy in generic B decays is about 200 MeV with a maximum energy above 4 GeV in some specific B decay modes. It is therefore mandatory to get a very low detection threshold ($\sim$ 20 MeV). Furthermore, excellent energy resolution over a large energy range is required to suppress the combinatorial background. These considerations have lead the collaboration to choose a calorimeter made of about 6800 CsI crystals read out by silicon photodiodes -presently the best calorimeter option. The depth of the crystals is gradually increased from 16.0 X_0 to 17.5 X_0 as one goes from the backward region to the forward end cap to match the boost of the particles. The expected performance of the calorimeter is briefly summarized in the figures 13 and 14. Such a device is operating very satisfactorily in the CLEO II detector.

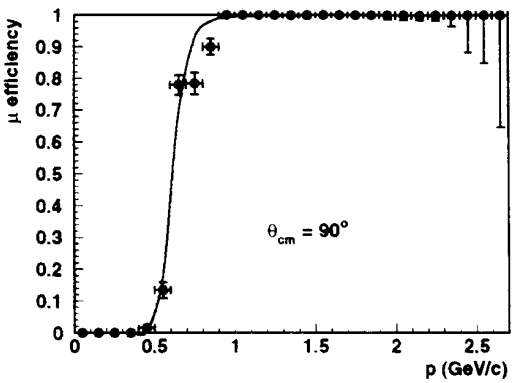

Figure 15: Efficiency for identifying muons with $\cos\theta_{cm} = 0$ as function of the muon momentum.

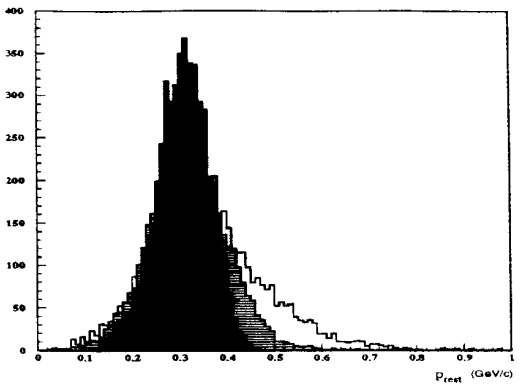

Figure 16: Reconstructed momentum of the B meson in the $\Upsilon(4S)$ rest frame for $B \to J/\psi K_L^0$ (dashed). The narrower distribution is due to the beam energy smearing while the broadest one shows the effect of removing the RPC layer inside the coil.

3.5 The instrumented flux return

Finally, as mentioned above, 17 layers of Resistive Plate Chambers[20] are used to instrument the flux return. Such chambers offer an efficient, robust and economical way for optimizing the acceptance coverage as demonstrated by operating experiments[15]. In addition to providing a very effective muon detection (fig. 15), this system allows one to reconstruct K_L^o and therefore to study the CP asymmetry in the mode $B \to J/\psi K_L^0$ (fig. 16).

4 – Conclusion

The *BABAR* detector provides a very promising tool to explore in detail the CP violation mechanism. It will allow us to make a comprehensive study of this phenomenon about 35 years after its discovery, possibly leading us toward new directions in particle Physics.

References

[1] A.D. Sakharov, Pis'ma Zh. Ekps. Teor. Fiz. **5** (1967) 32.

[2] J.H. Christenson, J.W. Cronin, V.L. Fitch and R. Turlay, Phys. Rev. Lett. **13** (1964) 138.

[3] *BABAR* Technical Design Report, SLAC-R-95-457, March, 1995.

[4] N. Cabibbo, Phys. Rev. Lett. **10** (1963) 531.

[5] B. Adeva et al, L3 Collaboration, Phys. Lett. B **231** (1989) 509;
D. Decamp et al, ALEPH Collaboration,, Phys. Lett. B **231** (1989) 519;

M.Z. Akrawy et al, OPAL Collaboration., Phys. Lett. B **231** (1989) 530;
P. Aarino et al, DELPHI Collaboration,, Phys. Lett. B **231** (1989) 539.

[6] M. Kobayashi and T. Maskawa, Prog. Theor. Phys. **42** (1973) 652.

[7] L. Wolfenstein, Phys. Rev. Lett. **51** (1983) 1945.

[8] J.M. Gerard, Plenary talk at the High Energy Physics conference of European Physical Society, Brussels, 7/27-8/2, 1995.

[9] R. Aleksan, Plenary talk at the High Energy Physics conference of European Physical Society, Brussels, 7/27-8/2, 1995.

[10] B. Kayser, M. Kuroda, R.D. Peccei and A.I. Sanda, Phys. Lett. B **237** (1990) 508; I. Dunietz, H. Quinn, A. Snyder, W. Toky and H.J. Lipkin, SLAC-PUB-5270, November 1990.

[11] R. Aleksan, A. Le Yaouanc, L. Oliver, O. Pene and J.C. Raynal, Phys. Lett. B **317** (1993) 173.

[12] R. Aleksan, I. Dunietz, B. Kayser, F. Le Diberder, Nucl. Phys. B **361** (1991) 141.

[13] see for example G.Batignani *et al.*, Nucl. Inst. and Meth. A **310** (1991) 160, Nucl. Inst. and Meth. A **320** (1992) 66.

[14] Y. Kubota *et al.*, Nucl. Inst. and Meth. A **320** (1992) 66.

[15] see for example A. Aloisio et al., Proceedings of the Sixth Pisa Meeting on Advanced Detectors, Isola d'Elba, Italy (1994), submitted to *Nucl. Instr. Methods*.

[16] S.M. Playfer, R. Bernet, R. Eichler and B. Stampfli, Nucl. Inst. and Meth. A **315** (1992) 494.

[17] A. Boyarski, D. Briggs and P. Burchat, Nucl. Inst. and Meth. A **323** (1992) 267.

[18] P. Coyle *et al.*, Nucl. Inst. and Meth. A **343** (1994) 292.

[19] G. Hamel de Monchenault and M. Zito, *BABAR* -DIRC note-1 ,July 1995.

[20] R. Santonico and R. Cardarelli, Nucl. Inst. and Meth. A **187** (1981) 377, Nucl. Inst. and Meth. A **263** (1988) 20.